International Conference on Mathematics, Computational Methods & Reactor Physics (M&C 2009)
Saratoga Springs, New York, May 3-7, 2009, on CD-ROM, American Nuclear Society, LaGrange Park, IL (2009)

STUDY OF THE PROMPT GAMMA RAY SIGNAL FROM FISSIONS IN SPECIAL NUCLEAR MATERIALS INDUCED USING AN ASSOCIATED PARTICLE NEUTRON GENERATOR

David. S. Koltick and Steven Z. Kane
Purdue University Applied Physics Laboratory
740 Navco Dr., Lafayette IN, 47905
koltick@purdue.edu, szkane@purdue.edu

ABSTRACT

More than 42 million cargo containers entered the United States in 2005 [1]. To search for a few kilograms of special nuclear material (SNM) within this vast stream of cargo, an inspection system based on neutron-induced fission followed by the coincident detection of multiple prompt fission gamma rays is investigated using MCNP-Polimi code. The system utilizes two deuterium-tritium (DT) associated particle neutron generators, each capable of 10^9 neutrons/s at 14.1 MeV, with sub-nanosecond timing resolution ZnO:Ga alpha detectors internal to the generator. Because prompt fission signals are approximately 100 times stronger than the delayed signals, the neutron flux is greatly reduced compared to $10^{11\text{-}12}$ neutrons/s [2, 3] required for systems based on delayed signals such as the "nuclear car wash" [4]. In addition the system utilizes 30 cm deep liquid krypton (LKr) noble gas detectors having 94% detection efficiency for 1 MeV gamma rays, high solid angle coverage (~ 50% of the total solid angle), and sub-nanosecond timing resolution (~ 600 ps) [5]. An algorithm for distinguishing U-235 from U-238 is presented.

Key Words: special nuclear material, prompt gamma rays

1. INTRODUCTION

The associated particle technique was developed by H. H. Barschall [6] in the early fifties and has been continuously developed since then [7-9]. In recent years, this technique has been utilized for the detection of explosives by numerous groups such as the EURITRACK project [10-12] and Andrey Kuznetsov *et. al*. [13, 14].

An associated particle neutron generator (APNG) enables the electronic collimation of the nearly isotropic distribution of neutrons that are emitted from deuterium-tritium fusion reactions created by accelerating a 50% mixture of deuterium and tritium ions onto a tritiated target [15]. Each reaction results in the emission of a 14.1 MeV neutron and 3.5 MeV alpha particle, which are correlated in time and travel in opposite directions to conserve momentum.

The APNG has a built-in position sensitive alpha detector, which provides directionality for the "tagged" neutrons. The resulting cone of tagged neutrons is used as a non-intrusive interrogation source. These neutrons interact producing a single gamma ray by neutron inelastic scattering or multiple gamma rays in the context of special nuclear material (SNM) by fast neutron-induced

fission. The neutron's time-of-flight can be obtained from the difference in the time of detection of an alpha particle and its correlated prompt gamma ray(s) [9]. Thus, the associated particle technique yields the 3-dimensional coordinates of the tagged neutron's interaction point [9]. The traditional approach is to use the tracking information to gate the gamma ray detectors to reduce background and to image the sample of interest [9].

Our intention is to use the sub-nanosecond timing information from the alpha detector to image or detect SNM by finding the origin of multiple coincident gamma rays.

2. THE CARGO INSPECTION SYSTEM

A schematic depiction of the modeled APNG system is shown in Figure 1. The detection system consists of two DT APNG such as Thermo Scientific A-920 [16, 17], each capable of producing 10^9 neutrons/s at 14.1 MeV, and 6 large area cylindrical liquid krypton (LKr) detectors each 1.2 m by 3 m and 30 cm deep. The goal is to segment the cargo container's cross section in time into nine 10 ns time gates and to segment the alpha detector into 16 pixels, yielding a total of 144 cross-sectional bins or "voxels" with a length of 30 cm for imaging.

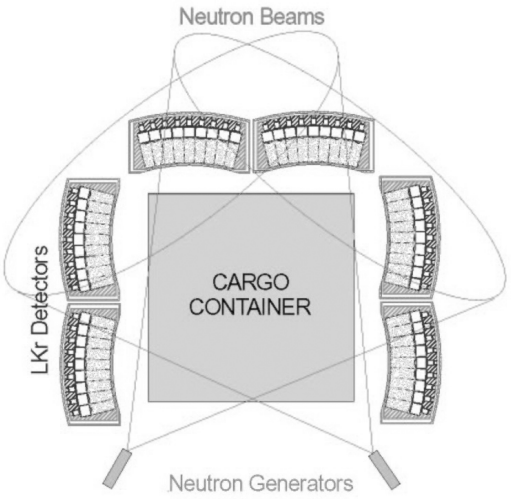

Figure 1. Proposed neutron interrogation system [18].

For this application, the probability of detecting fission events is proportional to the third or fourth power of detector efficiency, depending on the mode of detection. A good detection probability therefore requires detectors with several radiation lengths of depth. Liquid noble gas detectors match this application well because of their high stopping power, high detection efficiency, excellent radiation hardness, and sub-nanosecond timing capability [5]. Liquid xenon

(LXe) has a radiation length similar to NaI(Tl) but costs ~ 10 times more than liquid krypton. With a radiation length of 4.76 cm [19], krypton has a radiation length that is ~ 1.8 times longer than that of xenon's. Furthermore, it has been shown that a mixture of LKr and ~ 1% xenon provides practically the same scintillation properties as pure LXe [20, 21]. As shown in Figure 2, MCNP simulations indicate 30 cm deep LKr panels detect 1 MeV gamma rays with 94% efficiency.

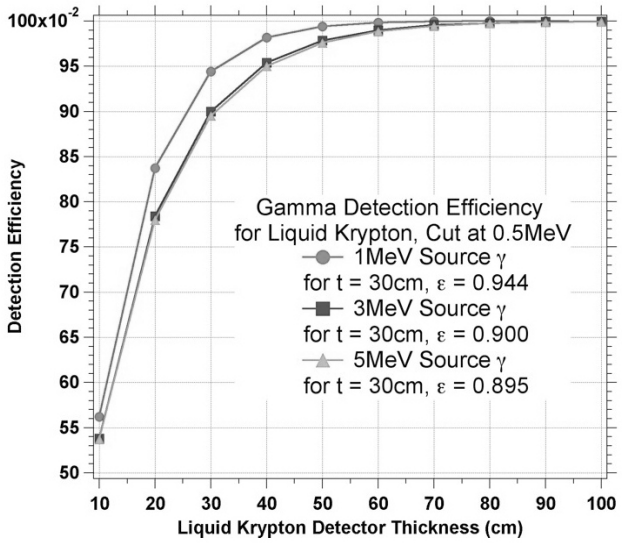

Figure 2. Simulation of liquid krypton detector efficiency using MCNP.

An A-920 APNG with active focusing has been produced and operated [16] using a ZnO:Ga alpha detector with large solid angle acceptance of 8%. The alpha detector's decay time, time resolution, and detection efficiency have been measured to be ~ 1 ns, ~ 500 ps, and ~ 88% [16], respectively. The neutron generator's DT beam spot has been measured down to 2.1 mm with the capability of achieving 1 mm if desired [16].

3. MODES OF DETECTION

Due to high-Z or charge of SNM, gamma rays exit a volume of SNM in a jet-like structure because those gamma rays that propagate inward away from the surface are absorbed, as shown in Figure 3. Therefore, a multi-level coincidence between adjacent panels is demanded which reduces background from random coincidences by a factor of 4. The system has two modes of detection: "fast fission" and "slow fission". As shown in Figure 4, the "fast fission" mode of detection is triggered by a coincidence between 3 adjacent LKr panels and the alpha particle associated with neutron production. "Fast fission" events are due to fission reactions caused by 14.1 MeV neutrons with fission cross sections of ~ 2 b [22] and ~ 1 b [23] for U-235 and U-238,

respectively. In this mode of detection, the location of the SNM is found using the associated particle technique. Knowing the position of an alpha particle, the direction and interaction point of its associated neutron is determined from the detection times of the alpha and correlated gamma rays.

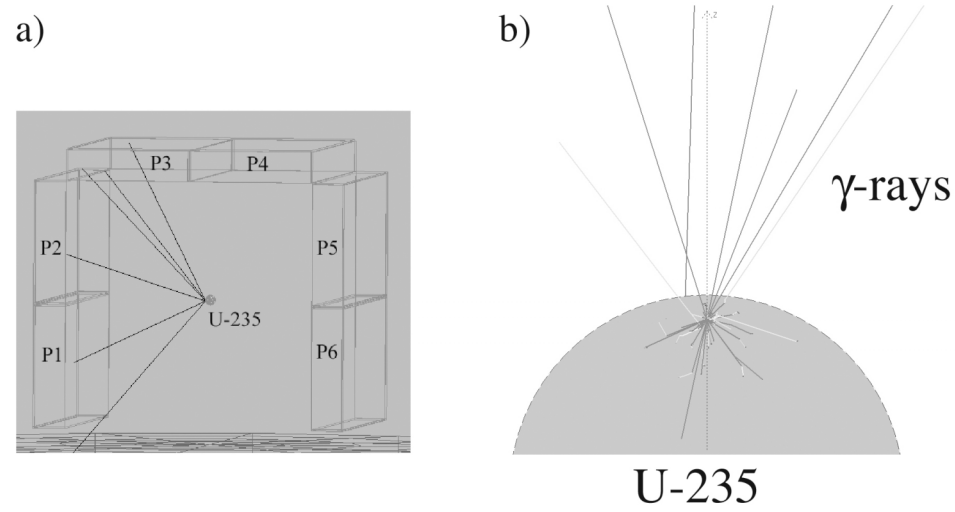

Figure 3. a) Coincidence event in detector panels P1, P2, and P3 due to prompt gamma rays from neutron-induced fission of U-235. The gamma rays escape in a "jet structure" due to self-attenuation of gamma rays traveling toward the center of the sample. b) Gamma ray emitted from fission event of U-235 from MCNP simulation.

As shown in Figure 5, the "slow fission" mode of detection is triggered by a coincidence between 4 adjacent panels and is assumed to be anti-coincident with the alpha particle associated with neutron production. These multiple coincident gamma ray events are due to fissions induced by slow thermal neutrons on U-235 with fission cross sections on order of 500 b [22]. As a fertile material, U-238 cannot be induced to fission by thermal neutrons. Consequently, the ratio of signals from fast and slow detection modes or 3-panel to 4-panel coincidences yields a method for distinguishing U-238 from U-235.

The first order trigger level SNM imaging is accomplished by assuming the center of a struck panel is the terminus of the gamma ray, regardless of the number of gamma rays hitting the panel. Then, given the relative timing of the detectors, a series of 1 ns arcs extending from each of the struck panels form a grid of curves, the intersection of which is the location of the SNM. Random coincidences will uniformly populate the cargo volume whereas the SNM will appear in a single voxel within the cargo.

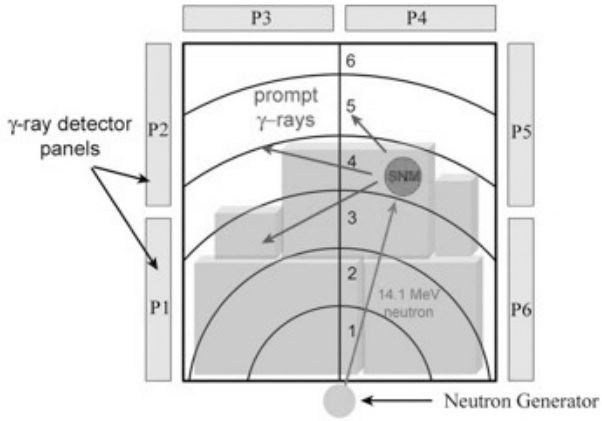

Figure 4. Fast fission event: a 14.1 MeV neutron initiates fission in SNM to produce a multi-gamma jet resulting in 3-fold coincidences in adjacent panels P1, P2, and P3 in coincidence with the alpha detector [18].

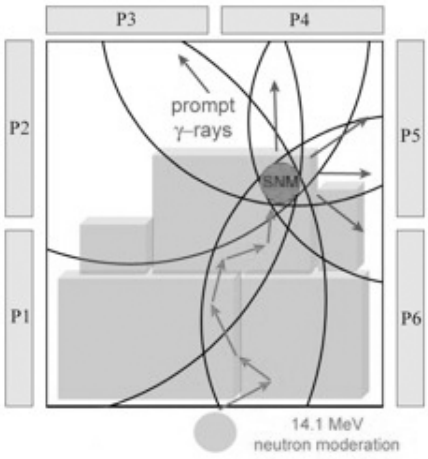

Figure 5. Slow fission event: a thermal neutron captures on U-235, resulting in 4-fold gamma ray coincidences in adjacent panels P3, P4, P5, and P6. The location of SNM is determined from the relative nanosecond timing of gamma rays in the LKr detectors [18].

4. MONTE CARLO SIMULATIONS

Simulations were performed using MCNP-Polimi version 1.0 [24]. The model geometry consisted of a 2.4 m x 2.4 m x 3 m steel cargo container resting on a concrete floor. The system's baseline performance was modeled using 5 kg spherical samples of U-235, U-238, and iron. . A 0.5 MeV threshold was applied to the LKr detector panels to eliminate annihilation photons and the Kr recoil events from n-elastic scattering. A 10 ns coincidence gate was utilized. All data reported are for a 30 cm cross section of a cargo container. The data were

obtained using 10^9 neutrons per second, which corresponds to less than one second of interrogation time. For the interrogation of a 40 foot-long cargo container, it is expected that approximately 10 times as much data would be collected due to higher neutron flux and longer interrogation time.

For an unshielded spherical sample centered in the cargo container, the expected panel coincidence rates for 3-fold and 4-fold coincidences were found to be 3 KHz and 800 Hz, respectively for U-235, and 850 Hz and 140 Hz, respectively for U-238. Expected coincidence rates for various shielded sample configurations, in which the entire container is uniformly filled with polyethylene or iron, are shown in Table 1.

Runs with iron samples have shown similar event topologies, producing both three and four panel coincidences. For 5 kg iron samples, the 3-fold coincidence rate observed is 1 kHz and the 4-fold coincidence rate is 150 Hz. In comparison with Table 1, these rates are comparable to 5 kg of U-238. These iron coincidence events are due to (n, γ) reactions which produce cascade de-excitations, resulting in the emission of several gamma rays within the 10 ns time gate. Iron has numerous energy states that can be excited by the neutrons. Other materials are expected to behave in a similar manner and are being investigated to understand how they may interfere with the identification of SNM.

Table 1. Expected coincidence rates using MCNP-Polimi.

Material	Configuration	3-Fold Rate R_3 (Hz)	4-Fold Rate R_4 (Hz)	Average Energy per Event (MeV)	Total Energy (MeV)	R_3/R_4
5 kg U-235	unshielded	3025	800	6	22862	~ 3.7
	0.1 g/cc plastic	704	121	5.5	4516	~ 5.8
	0.1 g/cc iron	1192	213	5.5	7677	~ 5.6
5kg U-238	unshielded	850	140	5.8	5707	~ 6
	0.1 g/cc plastic	144	14	5.5	872	~ 10.2
	0.1 g/cc iron	271	28	5.2	1563	~ 9.7
5kg Iron	unshielded	1026	152	4.7	5536	~ 6.7
	0.1 g/cc plastic	8	1	4	36	~ 8
	0.1 g/cc iron	37	5	3.9	164	~ 7.5

As shown in Figure 6, using two decision parameters the U-235 is distinguishable from U-238 and iron in all three cargo configurations. One of the decision parameters is the ratio of three-fold to four-fold coincidences measured in the sample's voxel. The other decision parameter is the product of the sum of the energy detected from all coincidence events originating from the

sample's voxel times the sum of coincidence count from that voxel. Note that the vertical dimension is in a logarithmic scale. The data show that the 5 kg samples of iron and U-238 are not distinguishable for a bare cargo container with these two decision parameters. As U-238 is not a SNM such identification is not a priority. However, in the presence of shielding material, the iron and U-238 separate within this decision hyperspace.

If it is desirable, U-238 can be separated from common materials. The three-fold coincidence rate in the case of U-238 is due to fast fission reactions, which do not occur for common materials. Fission of U-238 produces two excited nuclei. For this reason, we expect the average energy of the coincident gamma rays to be greater than those from cascade de-excitation of a simple nucleus. This is shown to be the case if we compare average event energies in each voxel shown in Table 1. Thus, by supplementing the decision space with an additional decision parameter, the average event energy in each voxel, U-238 can be separated from common materials, which produce coincident gamma ray cascades.

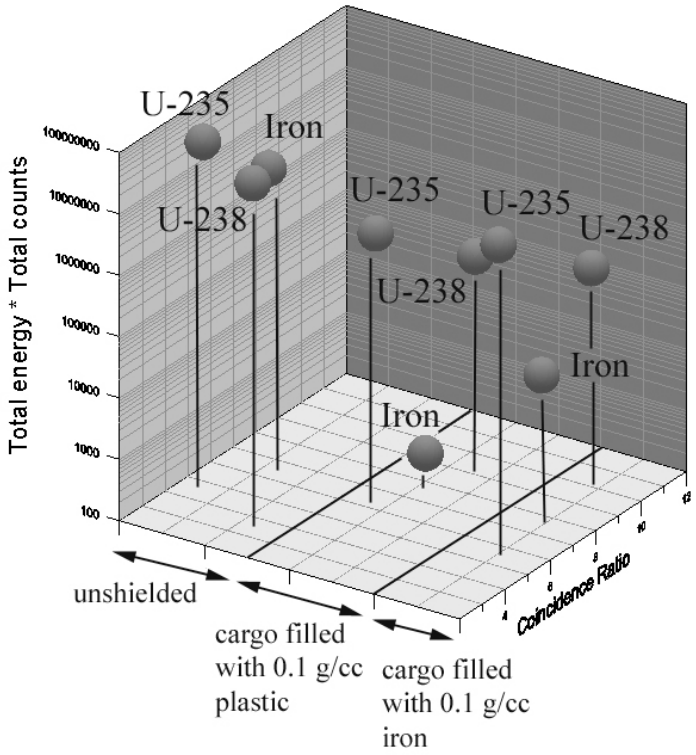

Figure 6. Hyperspace for SNM detection in bare cargo, cargo filled with plastic, and cargo filled with iron.

5. CONCLUSIONS

Monte Carlo simulations have been performed to study the use of prompt fission gamma rays as a signature for SNM. Coincidence rates were obtained for various shielded and unshielded cargo configurations. Two simple decision parameters were identified as the bases for a decision hyperspace. While cascade de-excitation is known to produce multiple coincident gamma rays in common materials, it was found that these materials separate from SNM in the decision hyperspace and from U-238 with an additional decision parameter. Experimental data has been obtained at Oak Ridge National Laboratory using an A-920 associated particle neutron generator. The experimental data is being analyzed for comparison with the MCNP predictions. Lastly, other cargo configurations and materials will be added to the SNM detection hyperspace.

REFERENCES

1. T. B. Cochran, M.G. McKinzie, "Detecting Nuclear Smuggling", Scientific American, April 2008, p.98.
2. J.M. Hall *et al.*, *Nucl. Instr. and Meth. B* **261**, 2007, 337-340.
3. D. Slaughter *et al.*, *Nucl. Instr. and Meth. B* **241**, 2005, 777-781.
4. D. Slaughter, *et al*., UCRL-ID 155315, Lawrence Livermore National Laboratory, Livermore, CA, August 2003.
5. D. Akimov *et al*., "Scintillating LXe/LKr Electromagnetic Calorimeter", IEEE Trans. Nucl. Sci. 1995, **42**, 2244-2249.
6. H. H. Barschall, L. Rosen, R.F. Taschek and J.H. Williams, *Rev. Mod. Phys.* **24** (1952) 1.
7. P.O. Hawkins and R.W. Sutton, *Rev. Sci. Instr.* **31** (1960), p. 241.
8. D.G. Shuster, *Nucl. Instr. and Meth*. **76** (1969) 35
9. E. Rhodes, C. Dickerman, M. Frey, "Advances in Associated-Particle Neutron Probe Diagnostics for Substance Detection", SPIE Vol. **2511**, 1995.
10. B. Perot *et. al*., *Nucl. Instr. and Meth. B* **261** (2007), p. 295.
11. S. Presente *et. al*., *Nucl. Instr. and Meth. B* **261** (2007), p. 268.
12. C. Carasco *et. al*., *Nucl. Instr. and Meth. A* **588** (2008), p. 397.
13. A. V. Kuznetsov, *et. al*. *Applied Radiation and Isotopes* **61** (2004), Issue 1, p. 51.
14. A.V. Kuznetsov, *et. al*. SENNA: device for explosives detection based on nanosecond neutron analysis, Proceedings of SPIE **6213** (2006).
15. Thermo Scientific, A-920 Neutron Generator Operator's Manual.
16. D. S. Koltick, S.Z. Kane, M. Lvovsky, E.K. Mace, S.M. McConchie, J.T. Mihalczo, "Characterization of an Associated Particle Neutron Generator with ZnO:Ga Alpha Detector and Active Focusing", Conference Proceedings Symposium on Radiation Measurements and Applications (Sorma West), 2008.
17. Thermo Scientific, Colorado Springs, CO 80919, USA.
18. D.S. Koltick, S.Z. Kane, "Cargo Inspection System for Special Nuclear Material (SNM) Based on Associated Particle Neutron Generators and Liquid-Kr detectors", Conference Proceedings 20th International *Conference on the Application of Accelerators in Research and Industry* (CAARI), 2008.

19. Journal of Physics G: Nuclear and Particle Physics, Vol. 33, July 2006, p. 104.
20. D. Akimov *et. al*., *Nucl. Instr. and Meth. A* **327** (1993), p. 155-158.
21. M. Chen *et. al*., *Nucl. Instr. and Meth. A* **327** (1993), p. 187-192.
22. National Nuclear Data Center, ENDF/B-VII.0: U-235(N,F).
23. National Nuclear Data Center, ENDF/B-VII.0: U-238(N,F).
24. E. Padovani and S. A. Pozzi, "MCNP-Polimi ver. 1.0 User's Manual", November 25, 2002.